

## 1 TITLE

2 Anatomical and isotopic traits in grapevine wood rings record environmental variability

3

## 4 SHORT TITLE

5 Wood anatomy and intrinsic water-use efficiency in grapevine

## 7 AUTHORS

8 Nicola Damiano<sup>1</sup>, Giovanna Battipaglia<sup>2</sup>, Paolo Cherubini<sup>3,4</sup>, Chiara Amitrano<sup>1</sup>, Simona  
9 Altieri<sup>2</sup>, Loïc Schneider<sup>3</sup>, Angela Balzano<sup>5</sup>, Chiara Cirillo<sup>1</sup>, Veronica De Micco<sup>1\*</sup>

## 11 ADDRESSES

12 <sup>1</sup> Department of Agricultural Sciences, University of Naples Federico II, via Università 100,  
13 80055 Portici (Naples), Italy

14 <sup>2</sup> Department of Environmental, Biological, Pharmaceutical Sciences and Technologies,  
15 University of Campania “Luigi Vanvitelli”, Via Vivaldi 43, 81100 Caserta, Italy

16 <sup>3</sup> WSL Swiss Federal Institute for Forest Snow and Landscape Research, Zürcherstrasse 111,  
17 CH-8903 Birmensdorf, Switzerland

18 <sup>4</sup> Department of Forest and Conservation Sciences, Faculty of Forestry, University of British  
19 Columbia, 2004-2424 Main Mall, V6T 1Z4, Vancouver BC, Canada

20 <sup>5</sup> University of Ljubljana, Biotechnical Faculty, Department of Wood Science and  
21 Technology, Ljubljana, Slovenia

22 This document is the accepted manuscript version of the following article:

Damiano, N., Battipaglia, G., Cherubini, P., Amitrano, C., Altieri, S., Schneider, L., ... De Micco, V. (2023). Anatomical and isotopic traits in grapevine wood rings record environmental variability. IAWA Journal. <https://doi.org/10.1163/22941932-bja10131>

23 \* Corresponding author

24 e-mail: demicco@unina.it

25

## Summary

In the Mediterranean region, prolonged droughts affect the growth, and reproductive cycles of grapevine. Changes in the physiological processes of grapevine, consequent to variations in environmental factors or cultivation management, are recorded in wood anatomical and isotopic traits in grapevine stems. In this study, we measured the anatomical traits and stable carbon isotope content in the annual rings of *Vitis vinifera* L. subsp. *vinifera* 'Falanghina' in four vineyards located in southern Italy, characterised by different water availability. The aim was to investigate how wood anatomical traits respond to interannual climatic variations according to local conditions.

Wood cores were taken from the stem of the grapevines and subjected to both microscopy and carbon stable isotope analyses to quantify functional wood anatomical traits, such as vessel size and frequency, and the intrinsic water-use efficiency of the grapevine. Wood traits were correlated with data of precipitation and temperature. The results showed that the plants at the four vineyards were characterised by different wood structure influencing grapevines physiology under different conditions of water availability. Overall, the analyses showed that the grapevines at the wetter sites developed wood traits, e.g., wide vessels, which favour the efficiency of water flow, while at the drier sites they developed plant traits, e.g., small vessels, which favour safety against embolism. However, the robustness of such main trends is trait-specific and is influenced by the interannual climatic variability.

## KEYWORDS

Carbon isotopes, drought, quantitative wood anatomy, *Vitis vinifera*, intrinsic water-use efficiency

## Introduction

The increase in frequency and severity of drought events in the Mediterranean region requires rapid and targeted adaptation of agricultural practices (Masson-Delmotte et al. 2021).

Grapevine (*Vitis vinifera* L. subsp. *vinifera*), in Italy predominantly grown in rainfed regime, is extremely interesting from a crop management perspective, as there is an increasing demand of cultivation techniques by stakeholders to improve the water stress tolerance to counteract the negative effects of climate change.

Plants hydraulic traits are affected by complex interactions among different environmental factors, as well as between environmental factors and cropping practices (Cirillo et al. 2017; Amitrano et al. 2019). Some cultivation techniques (e.g., canopy training system and pruning) directly influence crown structure, as shown by the allometric relationships with wood anatomical traits, and play an important role in controlling water-use efficiency (Cirillo et al. 2014, 2017; Souza et al. 2011; Willaume et al. 2004; Tyree & Evers, 1991). However, little is known about the role played by environmental factors, such as soil conditions, in the hydraulic architecture of grapevine xylem (Roig-Puscama et al. 2021). Grapevine vessel architecture and hydraulic characteristics are critical in the grapevine adaptation strategies, and must be considered in water management of the vineyard.

Variations in xylem vessel diameter and density are effective in changing plant responses to environmental conditions (Hacke et al. 2017a); indeed, small changes in the vessel lumen diameter are known to cause significant changes in the rate of xylem sap flow (Chavarria & dos Santos 2012; Hacke et al. 2017a, Pospíšilová & Zimmermann 1984). Grapevine has a ring-porous, sometimes semi-ring-porous wood, characterised by the presence of extremely large solitary vessels in the earlywood and narrow vessels grouped in radial rows or small groups in the latewood (Schweingruber 1990). Large vessels in the earlywood efficiently transport water, but they result not safe because of the risk of embolism under water stress

conditions (Hacke et al. 2006). Failure in the hydraulic system can occur for a variety of reasons, including frost and drought events (Tyree & Sperry 1989; Baas et al. 2004; Hacke et al. 2017b). For plant survival, it is mandatory that the reproductive and photosynthetic organs remain hydrated. Therefore, vessel cavitation may lead even to plant death due to extensive xylem embolism (Brodersen et al. 2010).

The ability to maintain a functioning hydraulic system during periods of drought ultimately depends on the ability of the vascular cambium to produce a hydraulic system adapted to the environmental fluctuations occurring at the plant growth site (Anderegg & Meinzer 2015; Hacke et al. 2001b; Hacke et al. 2017b; Islam et al. 2019). This ability is also reflected in the variation in vessel lumen size (Bittencourt et al. 2016; de Melo et al. 2018; Hacke et al. 2017b; Schmitz et al. 2006), which is influenced by several environmental factors, and determined by plant architecture (De Micco et al. 2008; Olson et al. 2014, 2018). Therefore, vessels traits, including size, distribution, and relationships with other cellular elements, provide valuable information for understanding how plants respond to environmental changes to which they are exposed (Robert et al. 2009). Stable carbon isotopes can help assess intrinsic water-use efficiency (iWUE) (Ehleringer et al. 1993), thus complementing the information gained from quantitative anatomy. Changes in iWUE are indeed very important because they reflect the rate of carbon assimilation and the loss of water to acquire CO<sub>2</sub>, thus the response to drought stress (Battipaglia et al. 2014; Altieri et al. 2015).

The aim of this study was to investigate the inter-annual and inter-site variability of the anatomical and isotopic (<sup>13</sup>C/<sup>12</sup>C) characteristics of xylem in the wood rings of grapevine grown in four vineyards with different environmental conditions in southern Italy. A previous study in the same vineyards has shown that grapevines have adapted their leaf anatomical traits, especially vein and stomata traits, in response to different pedoclimatic conditions, and that these traits correspond to different eco-physiological types (Damiano et al. 2022a).

Our hypothesis is that signs of acclimation observed in leaf anatomical traits in response to different environmental conditions may also be observed in the anatomical characteristics of the wood. In particular, we expect that under severe dry conditions wood anatomical traits adjust, as leaf anatomical traits do, to minimize embolism risk in the sites characterised by reduced water availability.

We also examined the relationships between wood traits and climatic factors to find possible triggers for traits favouring either the efficiency or the safety of the water transport system, likely reflecting different strategies for coping with drought at the four studied vineyards.

## Materials and methods

### *Study site and plant material*

Wood stem of *V. vinifera* subsp. *vinifera* 'Falanghina' (Controlled designation of origin – DOC/AOC) was collected in 2019 in 4 vineyards within the farm “La Guardiense” in southern Italy (Guardia Sanframondi, Benevento). The four vineyards are located at Santa Lucia (SL, 41° 14' 45" N; 14°34' 16" ,194 m a.s.l.), Calvese (CA, 41° 14' 19 N; 14° 35' 11"E, 163 m a.s.l.), Grottole (GR, 41°14' 21" N; 14°34' 56" E, 158 m a.s.l.), and Acquefredde (AC, 41° 13 ' 44" N; 14° 35' 33" E, 84 m a.s.l.). Grapevines ( $\approx$  4545 vines/ha) were grafted on 157-11 Couderc (*Vitis berlandieri*  $\times$  *Vitis riparia*) rootstock and were uniform for age, training system (double Guyot) and pruning management. The climate is Mediterranean with hot dry summer and wet mild winter. Meteorological data of the period 2015–2019 are from the Guardia Sanframondi weather station (41°14'17.2" N; 14°35'49.8" E) of the Campania region weather network ([www.agricoltura.regione.campania.it/meteo/agrometeo.htm](http://www.agricoltura.regione.campania.it/meteo/agrometeo.htm)). The average temperatures of the periods 21 June - 23 September and 21 December - 20 March of the five years were 25.2 °C and 9.3 °C, respectively. The mean cumulative precipitation of the periods 21 June - 23 September and 21 December - 20 March of the five years were 191 and 238 mm,

124 respectively. The following parameters were also considered: annual mean temperature  
125 (AMT), annual maximum temperature (AMaxT), annual minimum temperature (AMinT), and  
126 cumulative annual precipitation (CAP) (Table 1).

127 At the experimental sites, the soils are Mollisols, classified as Typic Calciustolls by the  
128 two principal soil series of the soil map of Valle Telesina area (1:50.000): i) Consociazione  
129 dei suoli Pennine (SL, CA and GR sites) and ii) Consociazione dei suoli Taverna Starze (AC  
130 site) (Terribile 1996). The horizons of the soil profiles are Ap and Bw, but the differences  
131 among the experimental sites are mostly due to the percentage of stones variability along the  
132 soil profile, and to the effect of vineyard planting. The four vineyards were cultivated under  
133 rainfed conditions. A supplemental irrigation, which is allowed only under particularly  
134 limiting conditions in specific years and is strictly regulated and controlled due to quality  
135 labels regulations, was applied at the AC site. Previous studies have indicated that the  
136 vineyards can be classified based on water availability for grapevines into two wetter sites,  
137 namely SL and AC, and two dryer sites, namely CA and GR (Damiano et al. 2022a, 2022b).  
138 Moreover, Damiano et al. (2022b) reported that in 2020 the cumulative precipitation was  
139 measured separately in each experimental vineyard showing that, in the period when high  
140 aridity is expected, CA and GR received almost halved water supply (18 and 15 mm)  
141 compared to SL (32 mm) and AC (9 mm + supplemental irrigation).

#### 142 *Sampling of wood-cores*

143 Wood cores of ten grapevines per vineyard were taken at the end of December 2019, from  
144 their main stem at a height of 20 cm above the graft union point, using a 0.5 cm Pressler  
145 increment borer. The 10 cores per each vineyard were first seasoned in a fresh-air dry store,  
146 then cross-sectioned, after rewetting the surface, for wood anatomical analysis, with a sliding  
147 microtome (WSL Core Microtome, Switzerland). Cross sections (13-15 µm thick) were

149 stained with a blend 1:1 of safranin (0.8 g in 100 ml distilled water) and Astra Blue (0.5 g in  
150 100 ml distilled water and 2 ml acetic acid). Then the microsections were washed with  
151 distilled water and subsequently dehydrated using an ethanol series from 40 to 100 % (Gartner  
& Schweingruber 2013) to be finally mounted with EUKITT® and dried in the oven at 50 °C  
for 24 hours.

#### *Wood-anatomical traits*

156 **Microphotographs of the cross sections from the ten cores** per vineyard were obtained with  
157 a digital slide scanner (Zeiss Axio Scan.Z1, Oberkochen, Germany) to obtain digital images at  
158 10x magnification and resolution of  $1300 \times 1030$  pixels for whole tree-ring series. Images  
were analysed to visually identify and date the rings. Digital images of whole rings of the last  
five years (2015-2019) **were captured in a selection of five cores per vineyard** with an EP50  
camera (Olympus, Hamburg, Germany) on a BX51 **transmitted** light microscope (Olympus,  
Hamburg, Germany). Images were analysed with the CellSens 3.2 (Olympus) software  
program. The following anatomical features were quantified in each ring: vessel area % (VA),  
ray area % (RA), fiber area % (FA) over the total section analysed, lumen area of each vessel,  
potential hydraulic conductivity (Kh) and hydraulic diameter (Dh) (Colangelo et al. 2017).  
More specifically, as described in Colangelo et al. (2017) the Kh was estimated as  $Kh = (\rho \times \pi \times \Sigma d^4) / (128 \times \mu \times Ar)$ , where “ $\rho$ ” is the density of water at 20 °C ( $998.2 \text{ kg m}^{-3}$ ), “d” is the  
vessel lumen diameter, “ $\mu$ ” is the viscosity of water ( $1.002 \times 10^{-9} \text{ MPa s}$  at 20 °C) and “Ar” is  
the area imaged; the Dh was calculated as the average of  $\Sigma d^5 / \Sigma d^4$ , where “d” is the medium  
Feret diameter of each vessel lumen. Considering that grapevine xylem, as other vines, is  
characterised by a large range of variation of vessel lumen area (VLA), in order to better  
analyse how different distributions of VLA are related to hydraulic properties, vessels were  
divided into three groups: lumen area  $< 500 \text{ } \mu\text{m}^2$  (A),  $500 \text{ } \mu\text{m}^2 < \text{lumen area} < 5000 \text{ } \mu\text{m}^2$  (B),



lumen area  $>5000 \mu\text{m}^2$  (C). Frequency distribution of the vessels in classes of lumen area within each group was calculated. In the three groups, the following parameters were quantified: average of minimum vessel area of group A (VAMin A), average of mean vessel area of group A (VAMean A), average of mean vessel area of group B (VAMean B), average of mean vessel area of group C (VAMean C), and average of maximum vessel area of group C (VAMax C).

### *Stable C isotope analysis*

After sectioning, the cores were observed under a dissection microscope Wild M32 (Leica, Wetzlar, Germany), in order to dissect single rings of the last five years, with a blade cutter. Each ring was ground in a centrifugal mill (ZM 1000, Retsch, Germany) with a 0.5-mm mesh size to ensure homogeneity. Stable C isotope composition ( $^{13}\text{C}/^{12}\text{C}$ ) was measured at the iCONa laboratory of the University of Campania (Caserta, Italy) by combustion in an elemental analyser (Flash EA 1112 series, Thermo Scientific, Waltham, MA, USA) connected via a CONFLO IV interface (Thermo Scientific, Waltham, MA, USA) to an isotope ratio mass-spectrometer (Delta V Advantage, Thermo Scientific, Waltham, MA, USA), operating in the continuous flow mode. Isotopic compositions are expressed in delta notation (‰) relative to an accepted reference standard: Vienna Pee Dee Belemnite for carbon isotope values. The standard deviation for the repeated analysis of an IAEA international standard (CH3, cellulose) was  $< 0.1\text{‰}$ . Finally, iWUE was estimated starting from the  $^{13}\text{C}$  isotope of the respective vineyards. In particular, a simplified version of the Farquhar et al. (1989) equation was used, excluding the mesophyll conductance of  $\text{CO}_2$  (Seibt et al. 2008) and post-photosynthetic processes that may potentially affect tree-ring  $\delta^{13}\text{C}$  (Gessler et al. 2014).

$$iWUE = \frac{ca(b - \Delta^{13}\text{C})}{16(b - a)}$$

With:

$$\Delta^{13}C = \frac{\delta^{13}C_{atm} - \delta^{13}C_p}{1 + \delta^{13}C_p}$$

where  $\Delta^{13}C$  is the photosynthetic discrimination against  $^{13}C$  in the atmosphere,  $\delta^{13}C_{atm}$  is the carbon isotope composition of atmospheric  $CO_2$ ,  $a$  is the mean annual atmospheric  $CO_2$  concentration,  $a$  is the fractionation during  $CO_2$  diffusion through stomata (44‰), and  $b$  is the fractionation during carboxylation (27‰),  $\delta^{13}C_p$  is the  $\delta^{13}C_p$  of each plant.

#### *Statistical analysis*

Shapiro–Wilk and Kolmogorov–Smirnov tests were performed to check for data normality. Logarithm transformation was applied in case data distribution was not normal. The percent data were previously subjected to arcsine transformation. Anatomical data were subjected to a two-way analysis of variance (ANOVA) using the four vineyards field (F) and year (Y) as main factors, and analysing their interaction ( $F \times Y$ ). Duncan’s multiple range test (at  $p \leq 0.05$ ) was applied to identify any significant differences among the four vineyards. iWUE data were analysed by one-way ANOVA, grouping the 5 years per core, and using F as factor. The SPSS 27 software package (SPSS Inc., Chicago, IL, USA) was used for the analyses.

**Correlations and multivariate analysis were performed** on anatomical, isotopic and climatic **data to visibly point out** relationships among variables which allow us to see patterns of data and understand multiple factors at once, making clear comparisons. To assess correlation between climatic and anatomical/isotopic data, the approach reported in Fritts (1976) for climate-growth relationships and used by Niccoli et al. (2020) was followed. More specifically, the climatic data of interest were divided by single or multiple months and were subjected to the linear Spearman’s correlation analysis to highlight the climatic parameter that have mostly influenced anatomical traits of *V. vinifera*. **Line plots, correlation plots (coreplot**

package with the Spearman's method) were performed using the R software environment for statistical computing and graphics (version 4.4.1).

Principal component analysis (PCA) was performed using Past3 statistical software (University of Oslo, Norway) as reported in Amitrano et al. (2021). PCA biplot analysis was used to find trends among variables (wood anatomical parameters) in the four vineyards, in order to minimize the number of non-independent variables into only two Principal Components (PC1 and PC2) which captures most of the variation.

## Results

Microscopy observations showed that the grapevines from the four vineyards were characterised by similar wood ring-anatomical characteristics (Fig. 1). Tree-ring boundaries were evident and typically undulating, and the wood was semi-ring or ring porous with wide parenchyma rays. In wide rings, the differentiation into earlywood, with very large vessels, and latewood, with very narrow vessels organized in radial files or small clusters, was evident. Such differentiation was less clear in narrow rings.

The effect of the main factor Y (Year) and of the interaction F (Field)  $\times$  Y were never significant in any anatomical parameters analysed. Concerning the area occupied by vessels, fibres and parenchyma cells in each tree ring, the main effect F was significant for VA (Vessel Area %) and FA (Fiber Area %). Concerning VA, the vineyard AC showed significantly higher values than SL and GR, with CA having intermediate values between AC and GR. The parameter FA was significantly higher in SL and GR sites compared to AC, with CA having intermediate values (Table 2).

As regards the mean vessel area calculated for the three VLA classes A, B and C (VAMean A, VAMean B, VAMean C), as well as the minimum and maximum vessel area calculated for the narrower (A) and larger (C) VLA classes, respectively (VAMin A,

VAMaxC), the main effect F was significant for all the analysed parameters except for

VAMean B. VAMin A and VAMean A showed the same trend of variation, with CA and AC reaching higher values than SL, which in turn had a significantly higher value than GR. VAMean C and VAMax C were significantly lower in GR compared to the other three vineyards (Table 3).

Finally, for the calculated potential hydraulic conductivity (Kh) and hydraulic diameter (Dh), the main effect of F was significant for narrower lumen area (KhA and DhA) and for the larger lumen area (KhC and DhC) groups, but not for the intermediate group (KhB and DhB). In particular, the vineyard GR showed significantly highest and lowest values of KhA and KhC, respectively, compared to the other vineyards. As regards the hydraulic diameter (Dh), GR showed DhA with the lowest value, whereas AC had the highest DhA. DhC was significantly lower in GR than in the other vineyards (Table 4).

The distribution of vessels in classes of lumen size within each of the groups A (lumen area  $<500 \mu\text{m}^2$ ), B ( $500 \mu\text{m}^2 < \text{lumen area} < 5000 \mu\text{m}^2$ ), and C (lumen area  $>5000 \mu\text{m}^2$ ) differed among the four vineyards (Fig.2). In particular, for the group A of lumen area, SL showed a tendency towards a higher frequency of lumen areas in the range  $350\text{-}500 \mu\text{m}^2$  and no vessels below  $200 \mu\text{m}^2$  (Fig. 2A). The field CA showed a tendency towards a higher incidence of lumen area in the range  $200\text{-}250 \mu\text{m}^2$  (Fig. 2D). GR showed the highest incidence of vessels in the class  $100\text{-}150 \mu\text{m}^2$  and was the sole vineyard to show vessels in the class  $50\text{-}100 \mu\text{m}^2$  (Fig. 2G). AC showed a vessel size distribution in the group A more similar to SL compared to the other two vineyards (Fig. 2L). For the distribution of vessels in the group B, the trends of lumen area distribution were similar among vineyards, with most of the water flow relying on vessels with lumen size in the range  $750\text{-}1750 \mu\text{m}^2$  (Fig. 2B, E, H, M). For the group C, all the vineyards with the exception of GR showed similar trends of VLA distribution, also with occurrence of vessels with  $\text{VLA} > 50000 \mu\text{m}^2$  (Fig. 2C, F, I, N). In GR,

most of the vessels showed lumen size in the range 7500-17500  $\mu\text{m}^2$  with no vessels above 42500  $\mu\text{m}^2$ . SL and AC sites showed a similar trend of the VLA distribution.

The carbon isotopes analyses indicated that values of iWUE at SL and AC sites were significantly lower than at CA and GR sites (Fig. 3).

In the multiple scatter plots (Fig. 4) the correlations among meteorological variables and wood traits are reported. In SL and CA, the iWUE was positively correlated with AMT, AMaxT and AMinT and negatively correlated with CAP. In GR, the iWUE was positively correlated with all the meteorological parameters. In GR, the KhA was negatively correlated with AMT, AMaxT and AMinT. The KhB in SL, CA and in GR was negatively correlated with AMT, AMaxT, AMinT and only in SL positively correlated with CAP. The KhC was negatively correlated with AMT, AMaxT and AMinT in SL, CA, AC and positively correlated with CAP. In GR, the KhC was positively correlated in AMT, AMaxT, AMinT and negatively with CAP. In the vineyard CA, the DhA was negatively correlated with AMT, AMaxT, AMinT and positively with CAP. DhB and DhC followed the same trends of correlations of KhB and KhC in the four vineyards. VA in the vineyards SL, CA, AC was negatively correlated with AMT, AMaxT, AMinT and positively correlated with CAP. RA was positively correlated with AMT, AMaxT, AMinT in the vineyards SL, CA, AC and negatively correlated in GR. RA was negatively correlated with CAP in SL and AC and was positively correlated with CAP in CA and GR. FA was negatively correlated with CAP in CA and GR positively with AMT, AMaxT, AMinT. VAMinA was negatively correlated with CAP in SL and AC and negatively correlated with AMT, AMaxT and AMinT in CA. VAMeanA was positively correlated with AMT, AMaxT, AMinT in SL and negatively with CAP in AC. VAMeanC and VAMaxC were positively correlated with AMT, AMaxT, AMinT in SL, CA and AC, and positively with CAP in SL and AC.

The PCA biplot (Fig. 5) separates the wood anatomical parameters and iWUE for the four vineyards SL, CA, GR, AC, during the five study years. The first two components explained a 64.29 % (PC1) and 23.26% (PC2) of the total variance, respectively. From the PCA, it is evident that the vineyard GR is the most different with reference to the other three, whereas, CA and AC sites are the most similar regarding wood characteristics particularly in the A lumen area class (widest vessels).

## Discussion

This study highlighted the variation of anatomical traits in the wood of ‘Falanghina’ grapevine grown in different vineyards. These variations are in line with different photosynthetic rates and productivity found in previous studies of the same vineyards (Damiano et al. 2022a, b, c), and suggest different water-use efficiency in the four vineyards in the five years analysed. In general, the four vineyards showed two main patterns of development of wood anatomical parameters and iWUE values. In particular, SL and AC were generally characterised by anatomical traits more focused on water flow efficiency and associated with lower iWUE. Low iWUE means that the plants assimilate less carbon per unit of water and thus that  $^{13}\text{CO}_2$  discrimination is high (Battipaglia et al., 2014). In contrast, GR showed anatomical traits safer against xylem embolism, which were associated with higher iWUE, suggesting lower  $^{13}\text{CO}_2$  discrimination, possibly due to partial or complete stomatal closure. CA showed intermediate behaviour, with anatomical traits more similar to SL and AC, while iWUE was closer to GR. The overall wood data are consistent with previous results from SL and AC, which were associated with higher water availability than vineyards at CA and GR sites (Damiano et al., 2022a, b). The efficiency of water transport is directly related to the plasticity of the vascular cambium (Hacke et al. 2017b; Islam et al. 2019; de Melo et al. 2018). This, in turn, leads to changes in vessel size (Hacke et

al. 2017b) when plants are affected by growth-limiting factors such as water shortage (de Melo et al. 2018; Schmitz et al. 2006) that triggers the formation of narrow vessels due to reduced turgor-induced enlargement during cell differentiation and as a strategy to reduce cavitation risk (Hacke et al. 2006; Roig-Puscama et al. 2021). Analysing the vessel size distribution among classes of diameter is important not only because variations in vessel size are indicators of possible constraints during cambial activity, but also because changes in vessel lumen can cause significant modification in the volume of xylem-sap flow (Hacke et al. 2017b). The larger the vessels, the higher is the impact on water flow, when even a small increase in vessel size occurs. While the analysis of larger vessels is important to obtain information on the efficiency of water flow, there is a growing awareness that very narrow vessels in grapevine must also be considered in any study aimed at understanding grapevine water flow and its ability to adapt to limited water availability. Indeed, a new paradigm has recently been established for grapevine, according to which xylem heterogeneity reduces flow rates in wider vessels by diverting 15% of total flow to narrow vessels, due to the occurrence of transverse pressure gradients (Bouda et al., 2019). Considering the data of VAMinA and the distribution of vessel size in the narrowest vessel lumen group (group A), the wood of GR shows narrower vessels compared to the other vineyards, especially SL and AC. On the other hand, the values of VAMeanC, VAMaxC and the distribution of vessel size in the group with the largest vessel lumen (group C) indicates that water flow in the wood of GR depends mainly on the size classes of vessel lumens up to a certain threshold, while the occurrence of very large vessels is limited compared to the other vineyards. Resistance to xylem embolism is related to a reduction in lumen area or mechanical reinforcement of fibres (Nardini et al. 2013). The heterogeneity of xylem in grapevines at the four sites is also reflected in Kh, which as well accounts for vessel frequency. The potential hydraulic conductivity Kh of the three classes A, B, and C was different in the four vineyards, indicating different water flow

strategies. In our case, the distribution between cell types (vessels, fibres, and parenchyma cells) was confirmed to be a rather stable feature between vineyards, suggesting that the mechanical resistance of wood does not vary significantly under different environmental conditions. Therefore, GR grapevines exhibit a stem vascular structure that would ensure a continuous, albeit slow, water flow under conditions of severe water shortage (Colangelo et al. 2017). On the contrary, under optimal temperature and rainfall conditions, grapevines at GR would still have lower performance compared to other vineyards. The different hydraulic behaviour of the wood, based on the anatomical and isotopic traits is consistent with leaf anatomical traits. Indeed, in previous studies (Damiano et al., 2022a, 2022b), grapevines at SL showed leaf vein and stomatal traits allowing the plants to keep stomata open to maintain high photosynthetic rates, regardless of increasing water losses through transpiration, even under conditions where grapevines at CA and GR promptly closed stomata to limit water loss through leaves (Damiano et al., 2022a). However, embolism risk in SL grapevines would also be limited due to other adaptations at the leaf anatomical level such as the appearance of narrower leaf veins, which are recognised to contribute to grapevine drought tolerance, and specific leaf venation controlling leaf hydraulic conductance (Broddrib et al., 2016; Creek et al., 2020; Dayer et al., 2020; Damiano et al., 2022a). In the SL and AC vineyards, the evapotranspiration needs of the grapevines seem to be continuously satisfied, in contrast to CA and GR, where the higher iWUE compared to SL and AC together with the overall quantitative anatomical data indicate that they were probably subjected to water shortage also in the years analysed (Damiano et al. 2022a). Stomatal closure during drought stress usually leads to an increase in iWUE (Altieri et al. 2015). This is consistent with the data obtained from the analysis of C isotopes in musts of the same grape varieties and with the low photosynthetic rate recorded in CA and GR (Damiano et al., 2022a, b). Grapevine wood combines the occurrence of frequent wide vessels, typical of grapevines, with high



heterogeneity in vessel size. This is a strategy that, under favourable environmental conditions, favours water transport efficiency while maintaining safety from embolism during drought as is the case of other Mediterranean woody species (Baas & Schweingruber, 1987; De Micco et al. 2008). The occurrence of different vessel size classes in a wood, also known as vessel dimorphism, is considered an adaptive trait to drought and is also a well-established ecological trend in wood anatomical characteristics (Baas & Schweingruber, 1987). The distribution of vessels in different classes of vessel lumen size can change in response to environmental changes, but also to local pedoclimatic conditions and cultivation practises (Cirillo et al. 2017). Comparing CA and GR, the two vineyards characterised by lower soil water availability, the wood traits of the CA vineyard (especially the wider range of vessel size distribution compared to GR) would explain the better growth performance of the first vineyard compared to the second, especially in drier years (Damiano et al. 2022a). The analysis of correlations between wood parameters and climatic data supports the idea of xylem plasticity triggered by temperature values and precipitation amount during the vegetative and reproductive seasons, but not with the same strength in all vineyards, as if local environmental conditions acted as a buffer. Thus, this analysis results fundamental in highlighting the differences among the four vineyards, supporting the data which were already discussed above. Indeed, iWUE positively correlated with all the temperature-related parameters (AMT, AMaxT, AMinT) in SL, CA and GR, and negatively with precipitation (CAP) in SL and CA. In the latter two sites, these results suggest that warm and dry conditions trigger wood-level adjustments that increase the amount of CO<sub>2</sub> fixed per transpired water, which is still ensured by a slow but continuous water flow thanks to a tendency to reduce the vessel size. This is also supported by the negative and positive correlations between the hydraulic conductivity of the classes with larger vessel lumens (KhB and KhC) and temperature and precipitation, respectively. Such trends are also quite

consolidated in other species as a typical response to dry conditions (Abrantes et al., 2013; Balzano et al., 2020). It is interesting to observe that at GR the correlation between iWUE and precipitation was positive, while increasing temperature would increase the incidence of water flow based on the classes of larger vessels (i.e., positive correlation between AMT, AMaxT and AMinT and KhC). Such a strategy might be possible in GR grapevines, as these plants can respond to severe drought by rapidly closing stomata due to their anatomical leaf characteristics, such as small and fast-responding guard cells (Damiano et al. 2022a). In the case of AC, relationships between climatic data and iWUE were not significant. In AC, the relationships between wood anatomical parameters and climatic data followed the same trends as in SL and CA, but were less marked. This is probably due to the cropping management allowing supplemental irrigation in case of severe drought, which may have buffered the relationships with temperature and precipitation data. In fact, according to Santesteban et al. (2012), AC vineyard would be classified as not affected by drought- stress based on  $\delta^{13}\text{C}$  values.

Our data show support that wood anatomical traits are likely modulated by environmental conditions during grapevine growth and can strongly influence the physiological responses of a grapevine cultivar to short-term changes in water availability, as iWUE indicated. The anatomical traits found in the four vineyards corresponding to spatial variation in environmental conditions indicated the occurrence of different water use strategies between the two wetter and the two drier sites. Trends in wood traits in the grapevines from the four vineyards were consistent with trends in leaf functional traits related to mesophyll and stomatal conductance highlighted in previous studies (Damiano et al. 2022a, b). Indeed, the importance of coordination between stomata and xylem traits for plant acclimation is also recognised at the evolutionary level (Brodribb et al., 2016). In a gradient of water availability,

SL is in the wettest end and so it functions as a water-spender (i.e. anisohydric), whereas GR is at the driest end and so it tends to be water-saving (i.e. isohydric).

In conclusion, our analyses support the idea that Falanghina grapevine can adopt different strategies of water use based on the development of specific structural traits at the wood and leaf levels, triggered by environmental conditions. Therefore, wood anatomical traits must be considered along with leaf hydraulic traits for a comprehensive understanding of grapevine water use, and for forecasting possible changes in the hydraulic behaviour under changing environmental conditions. Such an understanding would help develop science-based appropriate cultivation management techniques to promote grapevine acclimation to drought, especially with respect to precision application in viticulture.

## Acknowledgements

The work of Nicola Damiano was funded within the PhD Programme “Dottorati di Ricerca con Caratterizzazione Industriale”, P.O.R. CAMPANIA FSE 2014/2020. ASSE III—OBIETTIVO SPECIFICO 14 Azione 10.4.5. The authors wish to thank La Guardiense Farm (Guardia Sanframondi—BN) for technical support, Marco Giulioli, Concetta Pigna, Domizio Pigna and Arturo Erbaggio for support during the different phases of the project, and Antonello Bonfante for helpful support during the definition of the soils. The authors also wish to thank the owners of the vineyards for their logistic support: Antonello Foschini, Domenico Falluto, Marco Barbato and Domizio Pigna.

## References

Abrantes J, Campelo F, García-González I, Nabais C. 2013. Environmental control of vessel traits in *Quercus ilex* under Mediterranean climate: Relating xylem anatomy to function. *Trees* 27 (3): 655–662. DOI: 10.1007/s00468-012-0820-6

Altieri S, Mereu S, Cherubini P, Castaldi S, Sirignano C, *et al.* 2015. Tree-ring carbon and oxygen isotopes indicate different water use strategies in three Mediterranean shrubs at Capo Caccia (Sardinia, Italy). *Trees* 29 (5): 1593–1603. DOI: 10.1007/s00468-015-1242-z

Amitrano C, Arena C, Rouphael Y, de Pascale S, De Micco V. 2019. Vapour pressure deficit: The hidden driver behind plant morphofunctional traits in controlled environments. *Ann. Appl. Biol.* 175 (3): 313–325. DOI: 10.1111/aab.12544

Amitrano C, Arena C, Cirillo V, De Pascale S, De Micco V. 2021. Leaf morpho-anatomical traits in *Vigna radiata* L. affect plant photosynthetic acclimation to changing vapor pressure deficit. *Env. Exp. Bot.* 186, 104453. DOI:10.1016/j.envexpbot.2021.104453

Anderegg WRL, Meinzer FC. 2015. Wood anatomy and plant hydraulics in a changing climate. *Functional and Ecological Xylem Anatomy*, 235–253. Springer International Publishing; Switzerland. DOI: 10.1007/978-3-319-15783-2\_9

Alfonso VA, Baas P, Carlquist S, Chimelo JP, Coradin VT, *et al.* 1989. IAWA list of microscopic features for hardwood identification: With an Appendix on non-anatomical information. *IAWA J.* 10. 221-358. 10.1163/22941932-90000496.

Baas P, Schweingruber FH. 1987: Ecological Trends in the Wood Anatomy of Trees, Shrubs and Climbers from Europe. *IAWA J.* 8 (3): 245–274. DOI: <https://doi.org/10.1163/22941932-90001053>

Baas D, Aleman A, Kahn R. 2004. Lateralization of amygdala activation: A systematic review of functional neuroimaging studies. *Brain Res. Rev.* 45: 96–103. DOI: 10.1016/j.brainresrev.2004.02.004

Balzano A, Battipaglia G, Cherubini P, De Micco V. 2020. Xylem plasticity in *Pinus pinaster* and *Quercus ilex* growing at sites with different water availability in the mediterranean region: Relations between intra-annual density fluctuations and environmental conditions. *Forests* 11 (4) DOI: 10.3390/f11040379

Battipaglia G, De Micco V, Brand W A, Saurer M, Aronne G, *et al.* 2014. Drought impact on water use efficiency and intra-annual density fluctuations in *Erica arborea* on Elba (Italy). Plant Cell Environ. 37, 382–391. DOI: 10.1111/pce.12160

Bittencourt, PR, Pereira L, Oliveira RS. 2016. On xylem hydraulic efficiencies, wood space-use and the safety-efficiency tradeoff: comment on Gleason et al. (2016) 'Weak tradeoff between xylem safety and xylem-specific hydraulic efficiency across the world's woody plant species. New Phytol 211, 1152-1155. DOI: 10.1111/nph.14044

Bouda M, Windt C, McElrone A, Brodersen C. 2019. In vivo pressure gradient heterogeneity increases flow contribution of small diameter vessels in grapevine. Nat. Commun. 10: 5645. DOI: 10.1038/s41467-019-13673-6

Brodribb TJ, Bienaimé D, Marmottant P. 2016. Revealing catastrophic failure of leaf networks under stress. Proc Natl Acad Sci U S A 113 (17): 4865–4869. DOI: 10.1073/pnas.1522569113

Brodersen CR, McElrone AJ, Choat B, Matthews MA, Shackel KA. 2010. The Dynamics of Embolism Repair in Xylem: In Vivo Visualizations Using High-Resolution Computed Tomography. Plant Physiol. 154 (3): 1088–1095. DOI: 10.1104/pp.110.162396

Buesa I, Escalona JM, Tortosa I, Marín D, Loidi M, *et al.* 2021. Intracultivar genetic diversity in grapevine: Water use efficiency variability within cv. Grenache. Physiol Plant 173 (4): 2226–2237. DOI: 10.1111/ppl.13573

Chavarria G, dos Santos HP. 2012. Plant Water Relations: Absorption, Transport and Control Mechanisms. In: Montanaro G, Dichio B. (eds) Advances in Selected Plant Physiology Aspects:105-132. IntechOpen. DOI: 10.5772/33478

Cirillo C, De Micco V, Rouphael Y, Balzano A, Caputo R, *et al* 2017. Morpho-anatomical and physiological traits of two Bougainvillea genotypes trained to two shapes under deficit irrigation. Trees (Berl. West) 31 (1): 173–187. DOI: 10.1007/s00468-016-1466-6

- Cirillo C, Rouphael Y, Caputo R, Raimondi G, de Pascale S. 2014. The Influence of Deficit Irrigation on Growth, Ornamental Quality, and Water Use Efficiency of Three Potted Bougainvillea Genotypes Grown in Two Shapes. HortScience 49: 1284–1291. DOI: 10.21273/HORTSCI.49.10.1284
- Colangelo M, Camarero JJ, Battipaglia G, Borghetti M, de Micco V, *et al.* 2017. A multi-proxy assessment of dieback causes in a Mediterranean oak species. Tree Physiol. 37 (5): 617–631. DOI: 10.1093/treephys/tpx002
- Creek D, Lamarque LJ, Torres-Ruiz JM, Parise C, Burlett R, *et al.* 2020. Xylem embolism in leaves does not occur with open stomata: Evidence from direct observations using the optical visualization technique. J. Exp. Bot. 71 (3): 1151–1159. DOI: 10.1093/jxb/erz474
- Damiano N, Altieri S, Battipaglia G, De Micco V. 2022a. Comparing Methods for the Analysis of  $\delta^{13}\text{C}$  in Falanghina Grape Must from Different Pedoclimatic Conditions. Horticulturae 8 (3): 226. DOI: 10.3390/horticulturae8030226
- Damiano N, Arena C, Bonfante A, Caputo R, Erbaggio A, *et al.* 2022b. How Leaf Vein and Stomata Traits Are Related with Photosynthetic Efficiency in Falanghina Grapevine in Different Pedoclimatic Conditions. Plants 11 (11): 1507. DOI: 10.3390/plants11111507
- Damiano N, Cirillo C, Petracca F, Caputo R, Erbaggio A, Giulioli M, De Micco V. 2022c. Falanghina Grapevine (*Vitis vinifera* L.) Yield and Berry Quality under Different Pedoclimatic Conditions in Southern Italy. Horticulturae. 2022; 8(9):829. DOI: 10.3390/horticulturae8090829
- Davis SD, Sperry JS, Hacke UG. 1999. The relationship between xylem conduit diameter and cavitation caused by freezing. Am. J. Bot. 86 (10): 1367–1372. DOI: 10.2307/2656919
- Dayer S, Herrera J, Dai Z, Burlett R, Lamarque L, *et al.* 2020. The sequence and thresholds of leaf hydraulic traits underlying grapevine varietal differences in drought tolerance. J. Exp. Bot. 71 DOI: 10.1093/jxb/eraa186

- De Melo JCF, Amorim MW, Soffiatti P. 2018. Comparative wood anatomy of *Ficus*  
*cestrifolia* (Moraceae) in two distinct soil conditions. *Rodriguesia* 69 (4): 2109–2118. DOI:  
10.1590/2175-7860201869440
- De Micco V, Aronne G, Baas P. 2008. Wood anatomy and hydraulic architecture of stems  
and twigs of some Mediterranean trees and shrubs along a mesic-xeric gradient. *Trees* (Berl.  
West) 22 (5): 643–655. DOI: 10.1007/s00468-008-0222-y
- De Micco V, Aronne G. 2012. Morpho-Anatomical Traits for Plant Adaptation to Drought.  
In: Aroca, R. (eds) *Plant Responses to Drought Stress*. Springer, Berlin, Heidelberg.  
DOI:10.1007/978-3-642-32653-0\_2
- Ehleringer J, Hall A, Farquhar G. (eds) 1993. *Stable isotopes and plant carbon–water  
relations*. Academic Press, California, USA
- Farquhar GD, Ehlinger JR, Hubrick KT. 1989a. Carbon isotope discrimination and  
photosynthesis. *Annu. Rev. Plant Phys.* 40:503–537. DOI:  
10.1146/annurev.pp.40.060189.002443
- Francey RJ, Farquhar GD. 1982. An explanation of  $^{13}\text{C}/^{12}\text{C}$  variations in tree rings. *Nature*  
297: 28–31
- Fritts HC. 1976. *Tree Rings and Climate*. Academic, London, New York and San  
Francisco
- Gallo AE, Perez Peña JE, González CV, Prieto JA. 2022. Syrah and Grenache (*Vitis  
vinifera*) revealed different strategies to cope with high temperature. *Aust. J. Grape Wine Res.*  
28 (3): 383–394. DOI: 10.1111/ajgw.12530
- Gentilesca T, Battipaglia G, Borghetti M, Colangelo M, Altieri S, *et al.* 2021. Evaluating  
growth and intrinsic water-use efficiency in hardwood and conifer mixed plantations. *Trees*  
(Berl. West) 35 (4): 1329–1340. DOI: 10.1007/s00468-021-02120-z

- Gartner H, Schweingruber FH. 2013. Microscopic Preparation Techniques for Plant Stem Analysis. Kessel Publishing House, Remagen, Germany
- Gessler A, Ferrio JP, Hommel R, Treydte K, Werner RA, Monson RK. 2014. Stable isotopes in tree rings: towards a mechanistic understanding of isotope fractionation and mixing processes from the leaves to the wood. *Tree Physiol.* 34:796–818. DOI: 10.1093/treephys/tpu040
- Hacke U, Sperry J, Wheeler J, Castro L. 2006. Scaling of Angiosperm xylem structure with safety and efficiency. *Tree Physiol.* 26: 689–701. DOI: 10.1093/treephys/26.6.689
- Hacke UG, Sperry JS. 2001a. Functional and ecological xylem anatomy. *Perspect. Plant Ecol. Evol.* 4 (2): 97–115. DOI: <https://doi.org/10.1078/1433-8319-00017>
- Hacke UG, Sperry JS, Pockman WT, Davis SD, McCulloh KA. 2001b. Trends in wood density and structure are linked to prevention of xylem implosion by negative pressure. *Oecologia* 126 (4): 457–461. DOI: 10.1007/s004420100628
- Hacke UG, Sperry JS, Wheeler JK, Castro L. 2006. Scaling of angiosperm xylem structure with safety and efficiency. *Tree Physiol.* 26 (6): 689–701. DOI: 10.1093/treephys/26.6.689
- Hacke UG, Spicer R, Schreiber SG, Plavcová L. 2017a. An ecophysiological and developmental perspective on variation in vessel diameter. *Plant Cell Environ.* 40 (6): 831–845. DOI: <https://doi.org/10.1111/pce.12777>
- Hacke UG, Spicer R, Schreiber SG, Plavcová L. 2017b. An ecophysiological and developmental perspective on variation in vessel diameter. *Plant Cell Environ.* 40 (6): 831–845. DOI: <https://doi.org/10.1111/pce.12777>
- Islam M, Rahman M, Bräuning A. 2019. Impact of extreme drought on tree-ring width and vessel anatomical features of *Chukrasia tabularis*. *Dendrochronologia* 53: 63–72. DOI: 10.1016/j.dendro.2018.11.007



Lovisolo C, Hartung W, Schubert A. 2002. Whole-plant hydraulic conductance and root-  
 to-shoot flow of abscisic acid are independently affected by water stress in grapevines. *Funct.*  
*Plant Biol.* 29 (11): 1349–1356

Masson-Delmotte V, Zhai P, Chen Y, Goldfarb L, Gomis MI, *et al.* 2021. Working Group  
 I Contribution to the Sixth Assessment Report of the Intergovernmental Panel on Climate  
 Change. Geneva, Switzerland

Nardini A, Battistuzzo M, Savi T. 2013. Shoot desiccation and hydraulic failure in  
 temperate woody angiosperms during an extreme summer drought. *New Phytol.* 200 (2): 322–  
 329. DOI: 10.1111/nph.12288

Niccoli F, Pelleri F, Manetti MC, Sansone D, Battipaglia G. 2020. Effects of thinning  
 intensity on productivity and water use efficiency of *Quercus robur* L. *For. Ecol. Manag.* 473:  
 118282. DOI: 10.1016/j.foreco.2020.118282

Olson ME, Anfodillo T, Rosella JA, Petit G, Crivellaro A. *et al.* 2014. Universal  
 hydraulics of the flowering plants: Vessel diameter scales with stem length across angiosperm  
 lineages, habits and climates. *Ecology Letters* 17 (8): 988–997. DOI: 10.1111/ele.12302

Olson ME, Soriano D, Rosell J A, Anfodillo T, Donoghue MJ. *et al.* 2018. Plant height and  
 hydraulic vulnerability to drought and cold. *Proc. Nat. Acad. Sciences*, 115(29): 7551-7556.  
 DOI:10.1073/pnas.1721728115

Pospíšilová J, Zimmermann MH. 1984. Xylem Structure and the Ascent of Sap. *Biol.*  
*Plant.* 26 (3): 165. DOI: 10.1007/BF02895041

Robert EMR, Koedam N, Beeckman H, Schmitz N. 2009. A safe hydraulic architecture as  
 wood anatomical explanation for the difference in distribution of the mangroves *Avicennia*  
 and *Rhizophora*. *Funct. Ecol.* 23 (4): 649–657. DOI: 10.1111/j.1365-2435.2009.01551.x

Roig-Puscama F, Berli F, Roig F A, Tomazello-Filho M, Mastrantonio L, & Piccoli P  
 2021. Wood hydrosystem of three cultivars of *Vitis vinifera* L. is modified in response to  
 contrasting soils. Plant and Soil, 463(1): 573-588. DOI: 10.1007/s11104-021-04907-y  
 Santesteban LG, Miranda C, Urretavizcaya I, Royo J B. 2012. Carbon isotope ratio of  
 whole berries as an estimator of plant water status in grapevine (*Vitis vinifera* L.) cv.  
 ‘Tempranillo’. Sci Hortic. 146: 7–13. DOI: 10.1016/j.scienta.2012.08.006  
 Schmitz N, Verheyden A, Beeckman H, Kairo JG, Koedam N. 2006. Influence of a salinity  
 gradient on the vessel characters of the mangrove species *Rhizophora mucronata*. Ann. Bot.  
 98 (6): 1321–1330. DOI: 10.1093/aob/mcl224  
 Schweingruber FH. 1990. Anatomy of European woods : an atlas for the identification of  
 European trees, shrubs and dwarf shrubs. Verlag Paul Haupt, Bern.  
 Seibt U, Rajabi A, Griffiths H, Berry JA. 2008. Carbon isotopes and water use efficiency:  
 sense and sensitivity. Oecologia 155:441–454. DOI: 10.1007/s00442-007-0932-7  
 Souza JP, Prado CHBA, Albino ALS, Damascos MA, Souza GM. 2011. Network analysis  
 of tree crowns distinguishes functional groups of *Cerrado* species. Plant Ecol. 212 (1): 11–19.  
 DOI: 10.1007/s11258-010-9797-7  
 Terribile F, Gennaro AD, Mascellis RD. 1996. Carta dei suoli della Valle Telesina  
 (1:50.000). In Progetto UOT Relazione Finale Convenzione CNR-ISPAIM-Regione  
 Campania Assessorato Alla Agricoltura; Raccolta di 10 Carte Pedologiche della Regione  
 Campania  
 Tyree MT, Sperry JS. 1989. Vulnerability of Xylem to Cavitation and Embolism. Annu.  
 Rev. Plant Physiol. 40 (1): 19–36. DOI: 10.1146/annurev.pp.40.060189.000315  
 Tyree MT, Ewers FW. 1991. The hydraulic architecture of trees and other woody plants.  
 Tansley Review No. 34. New Phytol. 119: 345-360

615 Willaume M, Lauri P-É, Sinoquet H. 2004. Light interception in apple trees influenced by  
616 canopy architecture manipulation. *Trees* 18 (6): 705–713. DOI: 10.1007/s00468-004-0357-4

617

618

## FIGURE CAPTIONS

Fig. 1. Light microscopy views of cross sections of the trunk wood of grapevines from the four vineyards: Santa Lucia (SL); Calvese (CA); Grottole (GR); Acquefredde (AC).

Images are at the same magnification. Arrows indicate the beginning of the 2015 ring. Bars = 500  $\mu\text{m}$ .

Fig. 2. Distribution of vessels in classes of lumen area in the three groups A ( $<500 \mu\text{m}^2$ ), B ( $500 \mu\text{m}^2 < \text{lumen area} < 5000 \mu\text{m}^2$ ), C ( $>5000 \mu\text{m}^2$ ) in the trunk wood of grapevines from the four vineyards: A-C, Santa Lucia (SL); D-F, Calvese (CA); G-I, Grottole (GR); L-N, Acquefredde (AC).

Fig. 3. iWUE values in trunk wood (rings corresponding to the years from 2015 to 2019) of grapevines from the four vineyards (X-axis): Santa Lucia (SL); Calvese (CA); Grottole (GR); Acquefredde (AC). Mean values and standard errors are shown. Different letters corresponded to significantly different values according to Duncan HSD test ( $p < 0.001$ ).

Fig. 4. Spearman's rank correlation coefficients among climatic variables and wood anatomical traits in the four vineyards: Santa Lucia (SL); Calvese (CA); Grottole (GR); Acquefredde (AC). Positive (blue) and negative (red) correlations ( $r^2$ ) are shown. \*, \*\*, \*\*\*, significant at  $p < 0.05$ , 0.01 and 0.001 respectively.

Fig. 5. Principal component analysis (PCA) biplot showing relationships between wood anatomical parameters and iWUE among the four vineyards (Santa Lucia, SL; Calvese, CA; Grottole, GR; Acquefredde, AC) during the five years 2015-2019.

TABLES

**Table 1.** Climate data of the period 2015–2019 from the Guardia Sanframondi weather station (41°14’17.2” N;14°35’49.8” E) of the Campania region weather network: annual mean temperature (AMT), annual maximum temperature (AMaxT), annual minimum temperature (AMinT), and cumulative annual precipitation (CAP).

	AMT	AMaxT	AMinT	CAP
	°C	°C	°C	mm
2015	16.6	22.8	11.4	872
2016	16.5	22.9	11.3	931
2017	16.6	23.6	10.8	815
2018	16.8	22.8	12.0	1144
2019	17.3	23.0	12.1	821

**Table 2.** Main effects of field (F) and year (Y) on average of Vessel Area % (VA), Ray Area % (RA), Fiber Area % (FA) on ring area of *Vitis vinifera* L. subsp. *vinifera* ‘Falanghina’ from the four vineyards: Santa Lucia, SL; Calvese, CA; Grottole, GR; Acquefredde, AC. Mean values, standard errors and significance of main factors interactions are shown. Different letters within column indicate significant differences according to Duncan’s multiple-range test ( $P \leq 0.05$ ).

	VA %	FA %	RA %
<b>Field (F)</b>			
SL	22.82±1.244 c	43.03±0.655 a	36.61±0.957 a
CA	27.63±0.945 ab	40.60±0.729 ab	33.76±0.512 a
GR	24.55±0.828 bc	41.81±0.903 a	36.14±1.002 a
AC	29.84±1.613 a	39.40±1.348 b	34.25±1.107 a
<b>Year (Y)</b>			
2015	25.51±1.141 a	42.79±0.813 a	34.31±0.919 a
2016	25.49±1.254 a	42.12±0.988 a	35.19±0.851 a
2017	27.33±1.967 a	41.31±1.484 a	35.13±0.943 a
2018	26.83±1.241 a	39.86±1.120 a	36.33±0.968 a
2019	27.09±1.571 a	40.77±0.967 a	35.67±1.485 a
<b>Significance<sup>1</sup></b>			
F	***	**	NS
Y	NS	NS	NS
FxY	NS	NS	NS

<sup>1</sup>NS, \*, \*\*, \*\*\*: Non-significant or significant at  $P \leq 0.05$ , 0.01, 0.005, respectively.

**Table 3.** Main effects of field (F) and year (Y) on average of minimum Vessel Area of group A (VAMin A), average of mean vessel area of group A (VAMean A), average of mean Vessel Area of group B (VAMean B), average of mean Vessel Area of group C (VAMean C), average of maximum Vessel Area of group C (VAMax C) of *Vitis vinifera* L. subsp. *vinifera* ‘Falanghina’ from the four vineyards: Santa Lucia, SL; Calvese, CA; Grottole, GR; Acquefredde, AC. Mean values, standard errors and significance of main factors interactions are shown. Different letters within column indicate significant differences according to Duncan’s multiple-range test ( $P \leq 0.05$ ).

	VAMin A $\mu\text{m}^2$	VAMean A $\mu\text{m}^2$	VAMeanB $\mu\text{m}^2$	VAMeanC $\mu\text{m}^2$	VAMaxC $\mu\text{m}^2$
<b>Field (F)</b>					
SL	83.84±2.981 b	245.2±7.459 b	1377±46.84 a	17569±1066.5 a	31944±2373.3 a
CA	135.6±7.463 a	268.9±8.021 ab	1374±41.83 a	20530±1373.8 a	38101±2731.1 a
GR	49.91±3.637 c	195.5±7.792 c	1584±104.9 a	9903.2±694.9 b	16051±1518.1 b
AC	152.1±11.71 a	287.2±11.15 a	1376±43.77 a	18371±1054.7 a	34646±2208.1 a
<b>Year (Y)</b>					
2015	94.92±9.746 a	250.5±11.64 a	1392±65.69 a	16409±1398.5 a	29862±3181.3 a
2016	105.0±11.71 a	251.5±11.52 a	1443±58.00 a	16433±1700.2 a	30387±3437.4 a
2017	101.8±11.48 a	249.0±12.40 a	1432±53.51 a	15080±1056.2 a	28627±2401.1 a
2018	111.4±14.29 a	245.9±13.33 a	1375±63.35 a	19346±1787.5 a	34705±3479.6 a
2019	113.7±13.98 a	249.2±13.89 a	1500±117.1 a	15698±1344.7 a	27346±3056.5 a
<b>Significance<sup>1</sup></b>					
F	***	***	NS	***	***
Y	NS	NS	NS	NS	NS
FxY	NS	NS	NS	NS	NS

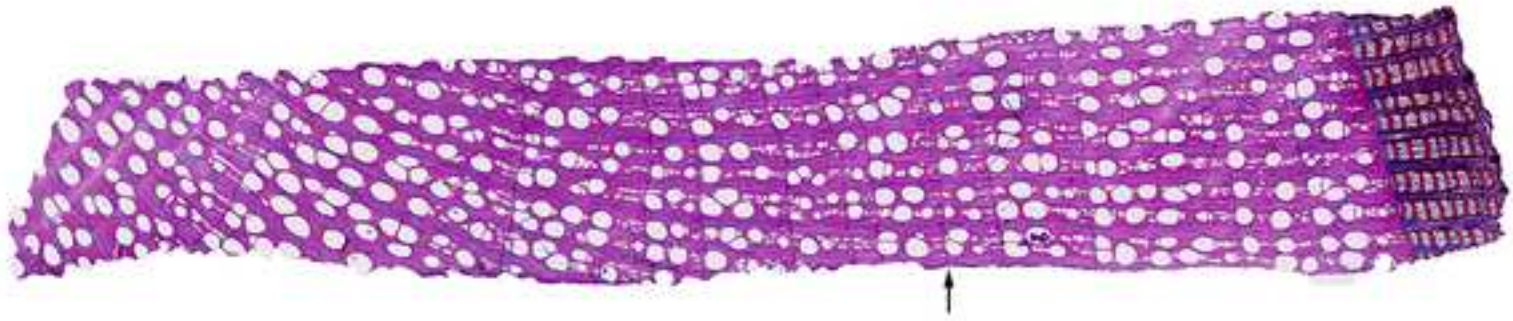
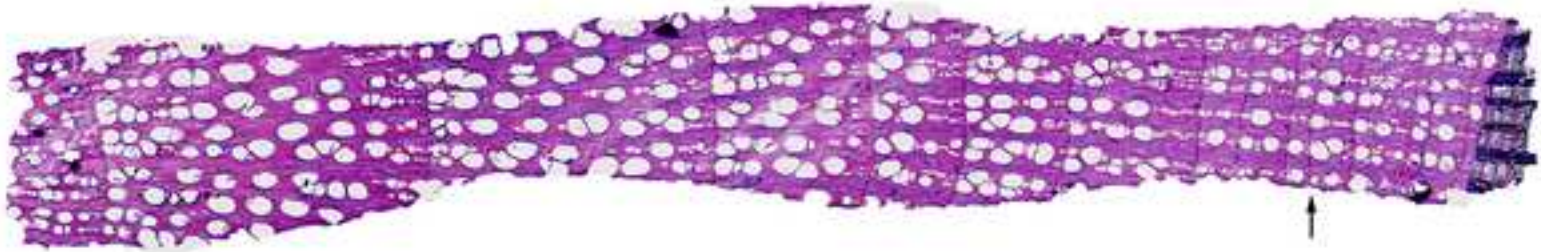
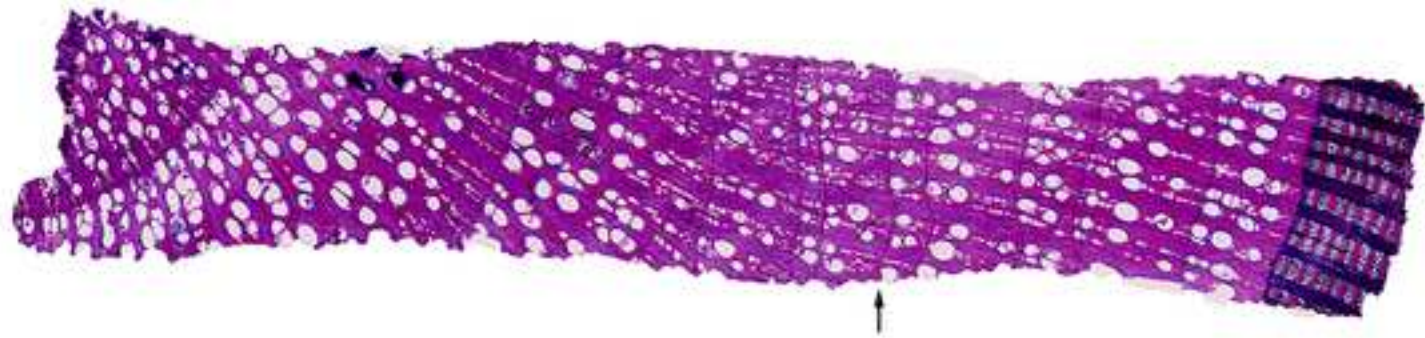
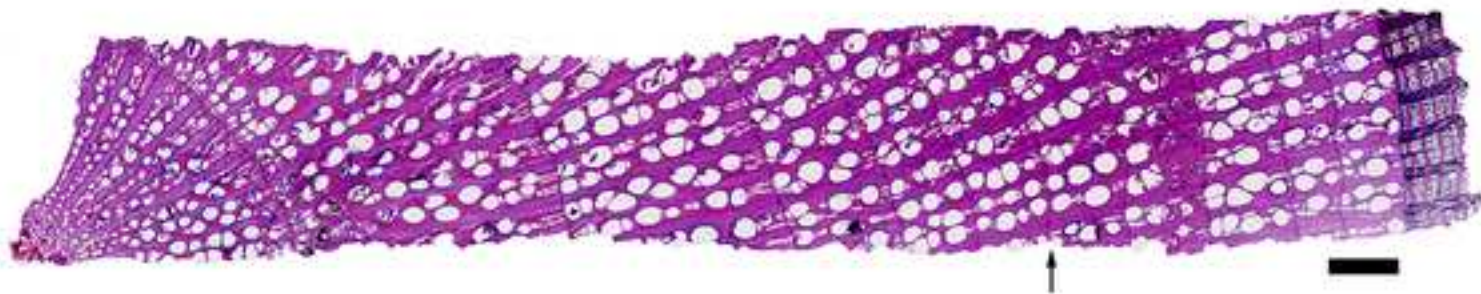
<sup>1</sup>NS, \*, \*\*, \*\*\*: Non-significant or significant at  $P \leq 0.05$ , 0.01, 0.005, respectively.

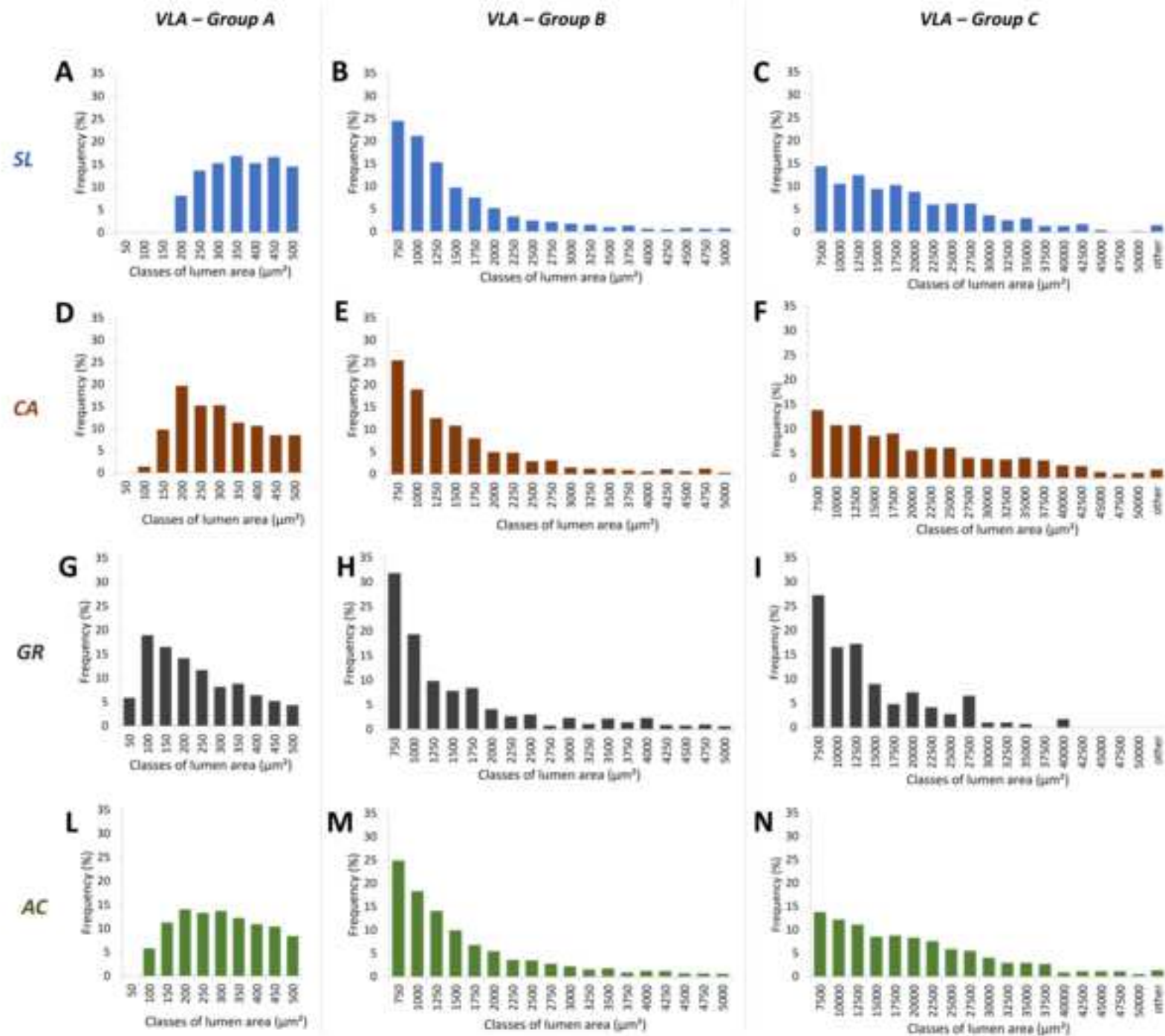
**Table 4.** Main effects of field (F) and year (Y) on potential hydraulic conductivity (Kh), hydraulic diameter (Dh), for the three group: lumen area <500  $\mu\text{m}^2$  (A), 500  $\mu\text{m}^2$  <lumen area<5000  $\mu\text{m}^2$  (B), lumen area >5000  $\mu\text{m}^2$  (C) of *Vitis vinifera* L. subsp. *vinifera* ‘Falanghina’ from the four vineyards: Santa Lucia, SL; Calvese, CA; Grottole, GR; Acquefredde, AC. Mean values, standard errors and significance of main factors interactions are shown. Different letters within column indicate significant differences according to Duncan’s multiple-range test ( $P \leq 0.05$ ).

	KhA ( $\text{kg m}^{-1}\text{MPa}^{-1} \text{s}^{-1}$ ) $\times 10^{-2}$	KhB ( $\text{kg m}^{-1}\text{MPa}^{-1} \text{s}^{-1}$ ) $\times 10^{-2}$	KhC ( $\text{kg m}^{-1}\text{MPa}^{-1} \text{s}^{-1}$ ) $\times 10^{-2}$	DhA $\mu\text{m}$	DhB $\mu\text{m}$	DhC $\mu\text{m}$
<b>Field (F)</b>						
SL	0.488 $\pm$ 0.074 b	10.68 $\pm$ 1.595 a	483.7 $\pm$ 159.1 a	34.05 $\pm$ 0.619 bc	76.51 $\pm$ 1.888 a	220.3 $\pm$ 7.642 a
CA	0.388 $\pm$ 0.046 b	7.168 $\pm$ 0.467 a	425.5 $\pm$ 41.54 a	36.54 $\pm$ 1.046 b	76.19 $\pm$ 1.188 a	239.9 $\pm$ 8.636 a
GR	0.782 $\pm$ 0.065 a	11.10 $\pm$ 1.628 a	158.1 $\pm$ 20.22 b	31.18 $\pm$ 0.863 c	76.57 $\pm$ 2.062 a	171.2 $\pm$ 7.720 b
AC	0.541 $\pm$ 0.052 b	9.729 $\pm$ 1.001 a	443.5 $\pm$ 66.84 a	40.41 $\pm$ 2.073 a	76.91 $\pm$ 1.707 a	221.8 $\pm$ 8.017 a
<b>Year (Y)</b>						
2015	0.588 $\pm$ 0.069 a	8.590 $\pm$ 1.072 a	348.4 $\pm$ 63.35 a	36.93 $\pm$ 2.154 a	76.84 $\pm$ 1.980 a	213.9 $\pm$ 9.948 a
2016	0.609 $\pm$ 0.097 a	10.27 $\pm$ 1.422 a	368.5 $\pm$ 79.67 a	36.92 $\pm$ 1.551 a	77.44 $\pm$ 1.597 a	212.4 $\pm$ 11.20 a
2017	0.487 $\pm$ 0.073 a	10.38 $\pm$ 1.329 a	286.9 $\pm$ 43.44 a	33.62 $\pm$ 0.999 a	78.36 $\pm$ 1.562 a	205.2 $\pm$ 8.886 a
2018	0.517 $\pm$ 0.062 a	9.711 $\pm$ 1.791 a	534.4 $\pm$ 186.6 a	36.74 $\pm$ 1.953 a	73.88 $\pm$ 1.890 a	231.3 $\pm$ 10.94 a
2019	0.549 $\pm$ 0.066 a	9.393 $\pm$ 1.574 a	350.3 $\pm$ 76.44 a	33.51 $\pm$ 0.877 a	76.22 $\pm$ 2.472 a	203.6 $\pm$ 11.32 a
<b>Significance<sup>1</sup></b>						
F	***	NS	*	***	NS	***
Y	NS	NS	NS	NS	NS	NS
FxY	NS	NS	NS	NS	NS	NS

<sup>1</sup>NS, \*, \*\*, \*\*\*: Non-significant or significant at  $P \leq 0.05$ , 0.01, 0.005, respectively.



**SL****CA****GR****AC**



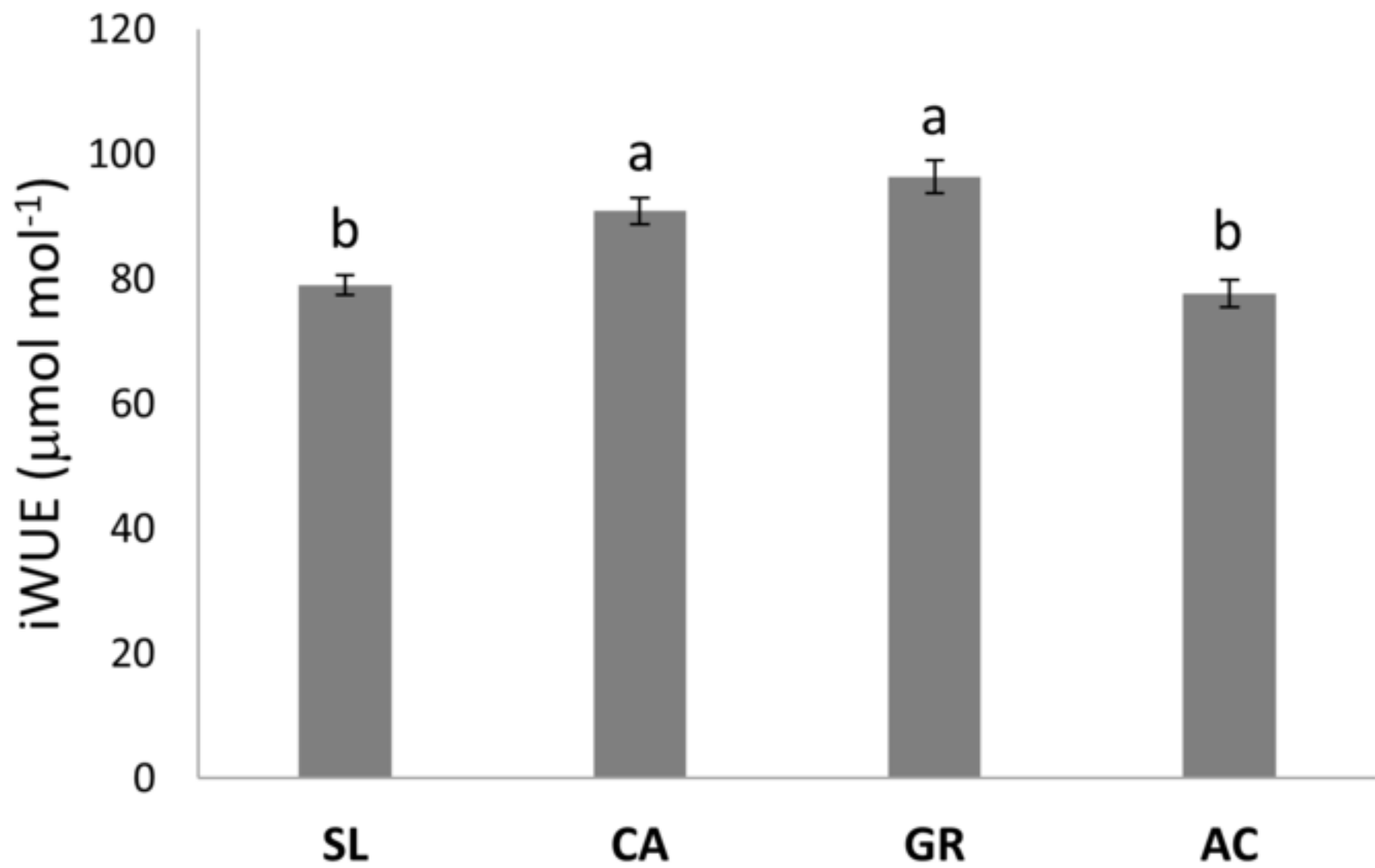




Figure 4

